Journal of Alloys and Compounds 522 (2012) 157–161

Contents lists available at SciVerse ScienceDirect

Journal of Alloys and Compounds

journal homepage: www.elsevier.com/locate/jallcom

Influence of zinc on electrical and microstructural properties of $CaCu_3Ti_4O_{12}$ ceramics prepared by sol–gel process

Dong Xu[a,b,c,*], Chen Zhang[a], Yuanhua Lin[d], Lei Jiao[a,e], Hongming Yuan[f], Guoping Zhao[a,e], Xiaonong Cheng[a,e]

[a] School of Material Science and Engineering, Jiangsu University, Zhenjiang 212013, PR China
[b] Key Laboratory of Semiconductor Materials Science, Institute of Semiconductors, Chinese Academy of Sciences, Beijing 100083, PR China
[c] State Key Laboratory of Electrical Insulation and Power Equipment, Xi'an Jiaotong University, Xi'an 710049, PR China
[d] State Key Laboratory of New Ceramic and Fine Processing(Tsinghua University), Beijing 100083, PR China
[e] Changzhou Engineering Research Institute of Jiangsu University, Changzhou 213000, PR China
[f] State Key Laboratory of Inorganic Synthesis and Preparative Chemistry, College of Chemistry, Jilin University, Changchun 130012, PR China

ARTICLE INFO

Article history:
Received 18 December 2011
Received in revised form 18 January 2012
Accepted 24 January 2012
Available online 2 February 2012

Keywords:
$CaCu_3Ti_4O_{12}$
Sol–gel
Dielectric properties
Varistor

ABSTRACT

Zn-substituted $CaCu_3Ti_4O_{12}$ ceramics were prepared by the sol–gel method. Their microstructures and electrical properties were investigated. XRD patterns showed that the $CaCu_{3-x}Zn_xTi_4O_{12}$ (CCZTO) ($x = 0.00, 0.06, 0.10, 0.20$) ceramics, after sintering at 1050 °C for 20 h, were single phase with no Cu-rich phase. SEM results indicated that the samples had smaller grain sizes than those synthesized by traditional solid-state reaction methods. The dielectric and varistor properties of CCZTO were analyzed by a precision impedance analyzer and a varistor tester, respectively. According to Debye's equation, which states that the smaller the leakage current, the smaller the dielectric loss will be in the low-frequency region, we were able to roughly predict the relative value of the dielectric loss at low frequency by the leakage current. The best overall properties were obtained for $x = 0.06$ ($CaCu_{2.94}Zn_{0.06}Ti_4O_{12}$), which has several prospective applications, such as low voltage varistor switchings, gas-sensing devices, and varistor–capacitor double property devices.

1. Introduction

Since the discovery of $CaCu_3Ti_4O_{12}$ (CCTO) ceramics by Subramanian et al. [1], considerable interest has been generated because of its very high dielectric constant, which is temperature- and frequency-independent in a wide range of temperatures near room temperature [1,2]. Homes et al. [3] have shown that the relative dielectric constant, ε_r, of single crystalline $CaCu_3Ti_4O_{12}$ is close to 10^5 at frequencies below 20 kHz at 250 K. With the miniaturization of memory devices and the improvement of devices integration, low-dielectric-constant materials who have low storage density are gradually becoming less suitable in the development process, and the electronics industry is in need of more applicable materials. CCTO is a promising material, and it is being considered as a candidate for applications in dynamic random access memory (DRAM) in very large scale integrated (VLSI) circuits due to its large dielectric constant [1–4]. Chung et al. have shown that $CaCu_3Ti_4O_{12}$ has an extremely strong nonlinear coefficient (α), which is much greater than that of ZnO, a typical varistor material [5]. Owing to these remarkable properties, CCTO has promising potential applications in capacitors, varistors, and their composites.

In spite of the wide variety of prospective applications, the nature and origin of the giant dielectric constant of CCTO ceramics remain controversial. Structural studies have showed that CCTO maintains a cubic structure without phase transitions down to 35 K [1]. Over the past few years, many theories have been proposed to describe the origin of the unusually high dielectric constant of CCTO, such as consideration of internal domains [6,7], the bimodal grain size model [8], electrode polarization effects [9], and so on. Among them, the internal barrier layer capacitor (IBLC) model, which considers CCTO as consisting of semiconducting grains with insulating grain boundaries [10,11], has been widely accepted. The nature of the Maxwell–Wagner relaxation in CCTO ceramics is well known [6].

Typically, the synthesis of CCTO ceramics follows a conventional solid-state reaction method [12,13]. Such as, Ni and Chen [14] used the solid-state reaction process to prepare the Zn-substituted CCTO ceramics. Hutagalung et al. [15] suggested using a new route, in which Zn-doped CCTO ceramics are produced by modified mechanical alloying technique. Although the process is able to produce high dielectric constant CCTO, the dielectric loss is relatively high. At

* Corresponding author at: School of Material Science and Engineering, Jiangsu University, Zhenjiang 212013, PR China. Tel.: +86 511 8879 7633.
E-mail address: frank@ujs.edu.cn (D. Xu).

0925-8388/$ – see front matter © 2012 Elsevier B.V. All rights reserved.
doi:10.1016/j.jallcom.2012.01.128

present, the sol-gel synthesis of CCTO ceramics and films is becoming increasingly popular [16–25]. Elemental substitution which can often change the crystal structure and electronic structure is a common method in materials research, it may be used to assist with the understanding of the origin of giant dielectric constant observed in CCTO ceramics. Due to the similarity in the size and the electronegativities of Zn and Cu, and in consideration of the homogeneity of the mixing process, the sol–gel method was adopted in this research in order to produce CCTO bulk materials with Zn substituted for Cu in the crystal lattice. Compared with some work on isovalent ion substitution for $CaCu_3Ti_4O_{12}$ that have been reported [14,15], the varistor properties, such as nonlinear coefficient, threshold field, and leakage current of Zn-doped CCTO ceramics have not been investigated, which also can be used to assist with the understanding of the origin of giant dielectric constant. Meanwhile, in our work, zinc oxide was added to CCTO by the sol–gel method to improve dielectric loss properties.

2. Experimental procedure

The sol–gel method was used to prepare the powders following a composition of $CaCu_{3-x}Zn_xTi_4O_{12}$ (CCZTO), for $x = 0.00$, 0.06, 0.10, and 0.20. Calcium nitrate ($Ca(CH_3COO)_2{\cdot}H_2O$), copper nitrate ($Cu(NO_3)_2{\cdot}3H_2O$), Zinc acetate($Zn(CH_3COO)_2{\cdot}2H_2O$)and tetrabutyl titanate ($Ti(OC_4H_9)_4$) were weighed according to the stoichiometric composition. $Ca(CH_3COO)_2{\cdot}H_2O$ and $Zn(CH_3COO)_2{\cdot}2H_2O$ were dissolved and mixed in distilled water with a small amount of nitric acid. $Cu(NO_3)_2{\cdot}3H_2O$ and $Ti(OC_4H_9)_4$ were both dissolved in ethanol. The Ca^{2+}, Zn^{2+} and Cu^{2+} precursor solutions were dropped into an acetic acid-stabilized titanium precursor and homogenized by magnetic stirring for 1 h, after which a blue-green transparent sol was obtained. This sol was allowed to age for 20 h at room temperature, and then the sol precursor was dried at 150 °C in an oven. Finally, the dried gel was decomposed at 900 °C for 10 h and pulverized to obtain the powders (powders labeled ZA0P, ZA1P, ZA2P, and ZA3P, respectively, for $x = 0$, 0.1, 0.2, 0.3, and 0.4). The calcined powders were then pressed into disks of 12 mm in diameter and 1.5 mm in thickness at a die pressure of 12 MPa. These disks were sintered in air at 1050 °C for 20 h (disks labeled ZA0, ZA1, ZA2, and ZA3, respectively, for $x = 0$, 0.1, 0.2, 0.3, and 0.4). The ramp rate was 5 °C/min. The ceramics were allowed to cool inside the furnace. Fig. 1 shows a flow chart of the bulk of CCZTO processing.

For the characterization of electrical properties, the silver paste was coated on both faces of samples and the silver electrodes were formed by heating at 600 °C for 10 min. The silver electrodes were a 5-mm diameter. The voltage–current (V–I) characteristics were measured using a V–I source/measure unit (CJP CJ1001). The nominal varistor voltages (V_N) at 0.1 and 1.0 mA were measured [26–29] and the threshold field V_T (V/mm) ($V_T = V_N(1\,mA)/d$; d is the thickness of the sample in mm).The leakage current (I_L) was measured at 0.75 V_N (1 mA). The measurement accuracy for voltage was ±0.5% and for electric current ±2%. In addition, the nonlinear coefficient α ($\alpha = 1/\log(V_{1.0\ mA}/V_{0.1\ mA})$) were determined with relative error of ±5% [27–34]. The dielectric characteristics, such as the apparent dielectric constant (ε) and dissipation factor (tan δ) at different frequencies were measured by an Agilent HP4294A impedance analyzer. The crystalline phases were identified by X-ray diffraction (XRD, Rigaku D/max 2500, Japan) analysis with Cu Kα radiation. The microstructures were evaluated by scanning electron microscopy (SEM, JEOL JSM-7001F) on the fractured surfaces.

3. Results and discussion

Fig. 2 shows the X-ray diffraction patterns of the CCZTO powders after calcining at 900 °C for 10 h. Compared to the major peaks of the CCTO spectrum, as found in the Powder Diffraction File database (PDF 21-0140), the diffraction peaks for the powders show that the CCTO phase formed, but a substantial portion of secondary phases ($CaTiO_3$, CuO and TiO_2) were also produced. The XRD patterns for the bulk CCZTO sintered at 1050 °C in air for 20 h are shown in Fig. 3. Similarities between the sintered and standard diffraction patterns suggest that the compounds are a single-phase CCTO structure. No secondary phases containing ZnO were detected up to $x = 0.20$, because XRD is not sensitive to concentrations under 0.5 wt.% [26–28,34–36]. The Zn ions were most likely substituted in Cu lattice sites [14]. These two occurrences are attributed to the lack of ZnO phases found in the CCZTO XRD spectra.

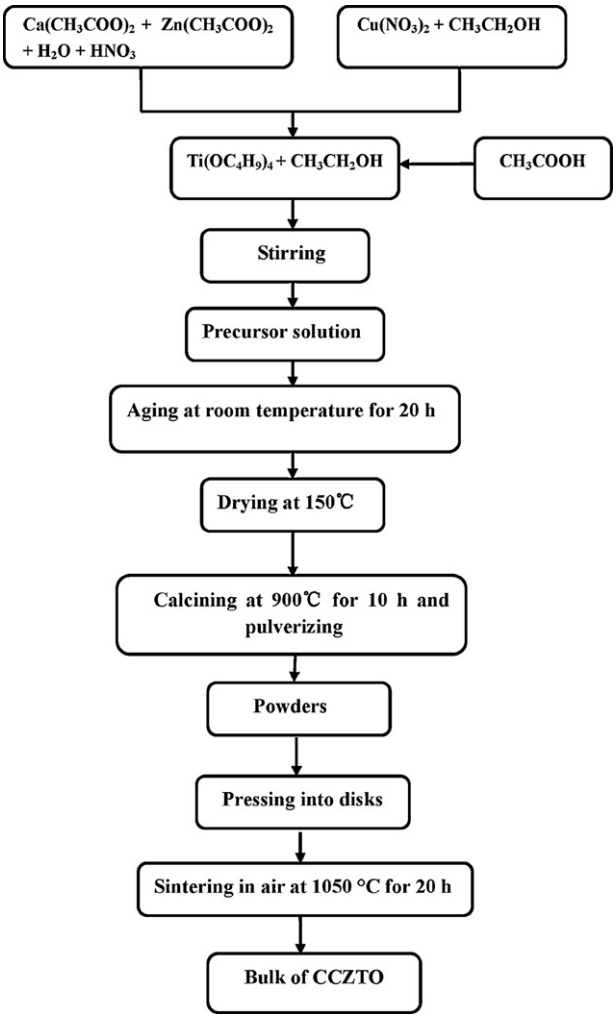

Fig. 1. Flow chart for the fabrication of CCZTO.

In Fig. 4, the SEM micrographs of newly fractured surfaces from the post-sintering samples are given. These images show that all the samples had a relatively homogeneous microstructure. There are no secondary phases observed in the undoped $CaCu_3Ti_4O_{12}$, such as a Cu-rich precipitate composition, as is often reported in the literature [13,37], and these are in line with the XRD analysis. The same average grain sizes were observed in samples of

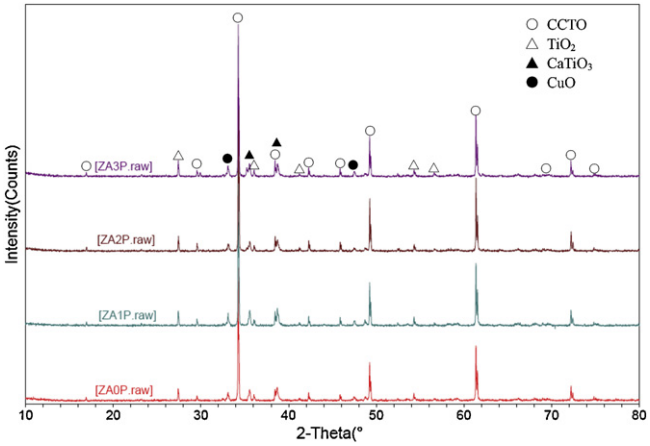

Fig. 2. XRD patterns for the calcined $CaCu_{3-x}Zn_xTi_4O_{12}$ ($x = 0.00$, 0.06, 0.10, 0.20) powders.

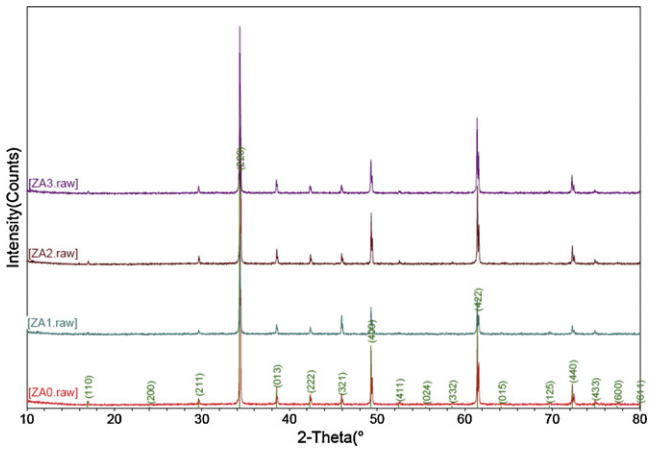

Fig. 3. XRD patterns of $CaCu_{3-x}Zn_xTi_4O_{12}$ ($x = 0.00, 0.06, 0.10, 0.20$) ceramics sintered at 1050 °C in air for 20 h.

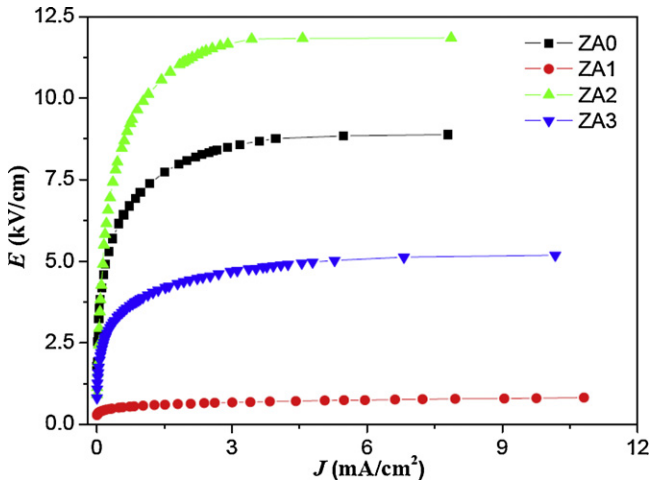

Fig. 5. Nonlinear E–J behaviors of $CaCu_{3-x}Zn_xTi_4O_{12}$ ($x = 0.00, 0.06, 0.10, 0.20$) ceramics.

$CaCu_3Ti_4O_{12}$ (the $x = 0.00$ sample), $CaCu_{2.9}Zn_{0.1}Ti_4O_{12}$ (the $x = 0.10$ sample), and $CaCu_{2.8}Zn_{0.2}Ti_4O_{12}$ (the $x = 0.20$ sample), which were approximately 2 μm. $CaCu_{2.94}Zn_{0.06}Ti_4O_{12}$ (the $x = 0.06$ sample) showed larger-sized grains (approximately 4 μm). In comparison to traditional solid-state reaction methods [13,37,38], smaller grain sizes can be obtained from samples which are synthesized by our sol–gel method.

Some slight differences can be observed in the micrographs. Some small white dots can be observed in the $CaCu_{2.9}Zn_{0.1}Ti_4O_{12}$ and $CaCu_{2.8}Zn_{0.2}Ti_4O_{12}$ images, which were not observed in the $CaCu_3Ti_4O_{12}$ and $CaCu_{2.94}Zn_{0.06}Ti_4O_{12}$ samples. According to the previous work [14], we believe that the small white dots are ZnO. With a small concentration of Zn ($x = 0.06$), the Zn ions will enter the lattice sites for Cu, and ZnO will form solid solution with CCTO; this helped promote grain growth and led to the larger grains in $CaCu_{2.94}Zn_{0.06}Ti_4O_{12}$. Because ZnO has a limited solubility in CCTO, and the amount of Zn ions that can replace Cu in the lattice is also finite [14,15], the surplus Zn ions may separate into extremely small crystals at the grain boundaries in the form of ZnO. Because of the higher melting point, the precipitated ZnO grains will result in grain boundary pinning and impede the growth of the CCTO grains.

Fig. 5 shows the electric field (E) versus current density (J) plots obtained for the samples. Due to the limitations of the experimental setup, when the voltages exceeded the breakdown values, the current values were not in compliance at 2 mA. Obviously, a strong nonlinear relationship between E and J is exhibited for all samples. The nonlinear coefficient values at room temperature were calculated for a current range of 0.1–1.0 mA for all samples, and can be found in Table 1. It was found that when $x = 0.06$, the highest

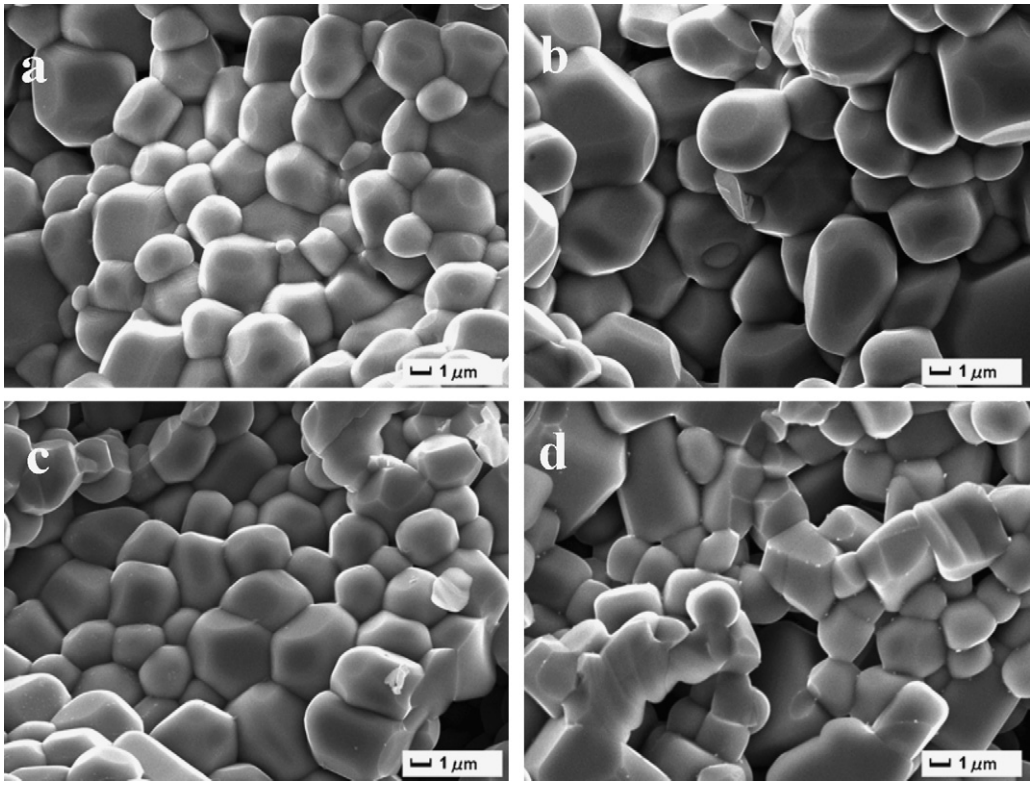

Fig. 4. SEM images of the newly fractured surfaces of $CaCu_{3-x}Zn_xTi_4O_{12}$ ceramics with (a) ZA0, (b) ZA1, (c) ZA2, and (d) ZA3.

Table 1
Nonlinear coefficient (α), threshold field (V_T), and leakage current (I_L) of $CaCu_{3-x}Zn_xTi_4O_{12}$ (x = 0.00, 0.06, 0.10, 0.20) ceramics.

Samples	α	V_T (V/mm)	I_L (μA)
x = 0.00	4.4	950	302
x = 0.06	6.4	76	162
x = 0.10	5.0	1220	175
x = 0.20	4.5	528	264

nonlinear coefficient (α = 6.4) was observed. With the addition of a small amount of Zn, there is a sudden improvement in the nonlinear coefficient, but with increasing concentrations, the nonlinear coefficient decreases. The threshold field (V_T) and leakage current (I_L) of the samples are also shown in Table 1. The $CaCu_{2.94}Zn_{0.06}Ti_4O_{12}$ showed the lowest threshold field and leakage current. Based on previous studies [39], the varistor capacitor characteristics in CCTO ceramics are associated with the grain boundary regions and correlated to the barrier height. We consider that a better insulativity of grain boundary and better electrical conductivity of gain can be obtained with bits of Zn (x = 0.06) substituting for Cu. This impurity helped improve the barrier height, such that $CaCu_{2.94}Zn_{0.06}Ti_4O_{12}$ had the highest nonlinear coefficient, α, and the lowest leakage current, I_L, among all the samples.

The frequency dependence of the dielectric constants (ε_r) and the dielectric loss factors (tanδ) at room temperature for the samples are shown in Fig. 6. It can be seen that the sample with x = 0.06

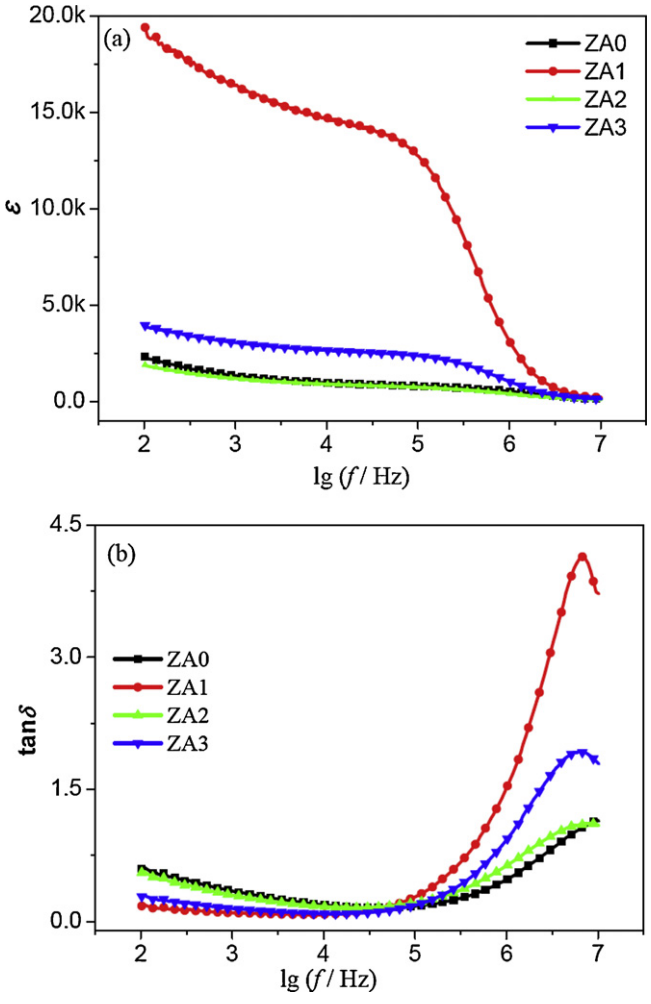

Fig. 6. Frequency dependence of (a) dielectric constants and (b) dielectric loss in $CaCu_{3-x}Zn_xTi_4O_{12}$ ceramics measured at room temperature.

has a much greater ε_r than other samples at frequencies below 10^5 Hz, after which a rapid reduction can be observed. Whereas the ε_r of the samples with x = 0.00, x = 0.10 and x = 0.20 remain almost unchanged, implying a good frequency stability, they are much smaller than that of $CaCu_{2.94}Zn_{0.06}Ti_4O_{12}$ (where x = 0.06). According to the literature [40], the dielectric constant of $CaCu_3Ti_4O_{12}$ is closely related to its grain size, and larger grains result in higher dielectric constants for $CaCu_3Ti_4O_{12}$. Our results lead to the same conclusion, whereby with larger grain sizes, a larger dielectric constant was observed for the $CaCu_{2.94}Zn_{0.06}Ti_4O_{12}$ case. With the internal barrier layer capacitor (IBLC) model [10,11,41], these results can be easily understood, as a greater amount of crystal defects are able to exist in larger grains than that in smaller ones. This allows for more internal barrier layers. The high dielectric constant of CCTO arises from the internal barrier layer capacitors, so a similar dielectric constant can be seen at every frequency for the samples where x = 0.00, x = 0.10, and x = 0.20 because of their similar grain sizes. In the low-frequency region, the $CaCu_{2.94}Zn_{0.06}Ti_4O_{12}$ has the lowest dielectric loss factor (0.0987 at 10^3 Hz), and a large increase in the loss factor occurs at frequencies greater than 10^5 Hz.

According to Debye's equation:

$$\tan\theta = \frac{(\varepsilon_{rs} - \varepsilon_{r\infty})\omega\tau}{\varepsilon_{rs} + \varepsilon_{r\infty}\omega^2\tau^2}$$

where tanθ is the polarization loss, ε_{rs} is the static dielectric constant, $\varepsilon_{r\infty}$ is the optical dielectric constant, ω is the angular frequency, and τ is the relaxation time. When the frequency is low, ω converges to zero and tanθ is very small (also converges to zero). In the low-frequency region, the loss (tanδ) is mainly caused by the leakage current. With this information, we see that the smaller the leakage current, the smaller the dielectric loss at low frequency that can be obtained when other factors are ignored. Correlating Fig. 6 with Table 1, not including $CaCu_{2.9}Zn_{0.1}Ti_4O_{12}$ (the sample where x = 0.10), all the samples are in accord with this law. There must be some other significant factors influencing the dielectric loss in $CaCu_{2.9}Zn_{0.1}Ti4O_{12}$, which require a further research.

4. Conclusions

Synthesis of CCZTO by the sol–gel method was performed using precursors of $Ca(CH_3COO)_2{\cdot}H_2O$, $Cu(NO_3)_2{\cdot}3H_2O$, $Zn(CH_3COO)_2{\cdot}2H_2O$, and $Ti(OC_4H_9)_4$. XRD analysis indicated that the samples consisted of a single phase, with no secondary phases. From SEM observations, we found that some ZnO grains appeared on the grain boundaries in $CaCu_{2.9}Zn_{0.1}Ti_4O_{12}$ and $CaCu_{2.8}Zn_{0.2}Ti_4O_{12}$, which led to grain confinement in the CCTO. Furthermore, along with the dielectric measurements, previous reports of larger grain sizes resulting in higher dielectric constant for $CaCu_3Ti_4O_{12}$ were verified. Overall, it was found that $CaCu_{2.94}Zn_{0.06}Ti_4O_{12}$ (the sample with x = 0.06) had the best properties, with the highest nonlinear coefficient, the lowest threshold field, a high dielectric constant, and a low dielectric loss factor at frequencies below 10^5 Hz. These properties make it a candidate for applications in low voltage varistor switchings, gas-sensing devices, and varistor–capacitor double property devices. To widen its application area, further studies are needed to increase its nonlinear coefficient, to stabilize the dielectric constant, and to reduce the dielectric loss factor in the high-frequency region.

Acknowledgments

This work was financially supported by the Natural Science Foundation of Jiangsu Province (BK2011243), Research Foundation of Jiangsu University (11JDG084), Opening Project of State key Laboratory of Electronic Thin Films and Integrated Devices

(KFJJ201105), Leading Academic Discipline Project of Shanghai Municipal Education Commission (J50102), State Key Laboratory of Inorganic Synthesis and Preparative Chemistry of Jilin University (2011-22), State Key Laboratory of New Ceramic and Fine Processing Tsinghua University (KF201104), State Key Laboratory of Electrical Insulation and Power Equipment (EIPE11204) and Universities Natural Science Research Project of Jiangsu Province (10KJD430002).

References

[1] M.A. Subramanian, D. Li, N. Duan, B.A. Reisner, A.W. Sleight, J. Solid State Chem. 151 (2000) 323–325.
[2] A.P. Ramirez, M.A. Subramanian, M. Gardel, G. Blumberg, D. Li, T. Vogt, S.M. Shapiro, Solid State Commun. 115 (2000) 217–220.
[3] C.C. Homes, T. Vogt, S.M. Shapiro, S. Wakimoto, A.P. Ramirez, Science 293 (2001) 673–676.
[4] L.C. Chang, D.Y. Lee, C.C. Ho, B.S. Chiou, Thin Solid Films 516 (2007) 454–459.
[5] S.Y. Chung, I.D. Kim, S. Kang, Nat. Mater. 3 (2004) 774–778.
[6] T.T. Fang, L.T. Mei, J. Am. Ceram. Soc. 90 (2007) 638–640.
[7] T.T. Fang, C.P. Liu, Chem. Mater. 17 (2005) 5167–5171.
[8] M.J. Pan, B.A. Bender, J. Am. Ceram. Soc. 88 (2005) 2611–2614.
[9] P. Lunkenheimer, R. Fichtl, S.G. Ebbinghaus, A. Loidl, Phys. Rev. B. (2004) 70.
[10] D.C. Sinclair, T.B. Adams, F.D. Morrison, A.R. West, Appl. Phys. Lett. 80 (2002) 2153–2155.
[11] T.B. Adams, D.C. Sinclair, A.R. West, Adv. Mater. 14 (2002) 1321.
[12] G. Du, W. Li, Y. Fu, N. Chen, C. Yin, M. Yan, Mater. Res. Bull. 43 (2008) 2504–2508.
[13] T. Li, Z.P. Chen, Y.L. Su, L. Su, J.C. Zhang, J. Mater. Sci. 44 (2009) 6149–6154.
[14] L. Ni, X.M. Chen, J. Am. Ceram. Soc. 93 (2010) 184–189.
[15] S.D. Hutagalung, L.Y. Ooi, Z.A. Ahmad, J. Alloys Compd. 476 (2009) 477–481.
[16] D.L. Sun, A.Y. Wu, S.T. Yin, J. Am. Ceram. Soc. 91 (2008) 169–173.
[17] L. Liu, H. Fan, P. Fang, X. Chen, Mater. Res. Bull. 43 (2008) 1800–1807.
[18] R. Parra, R. Savu, L.A. Ramajo, M.A. Ponce, J.A. Varela, M.S. Castro, P.R. Bueno, E. Joanni, J. Solid State Chem. 183 (2010) 1209–1214.
[19] R. Jimenez, M.L. Calzada, I. Bretos, J.C. Goes, A. Sombra, J. Eur. Ceram. Soc. 27 (2007) 3829–3833.
[20] J. Li, T. Xu, S. Li, H. Jin, W. Li, J. Alloys Compd. 506 (2010) L1–L4.
[21] T. Li, R. Xue, J. Hao, Y. Xue, Z. Chen, J. Alloys Compd. 509 (2011) 1025–1028.
[22] J. Lu, D. Wang, C. Zhao, J. Alloys Compd. 509 (2011) 3103–3107.
[23] M. Oghbaei, O. Mirzaee, J. Alloys Compd. 494 (2010) 175–189.
[24] L. Ramajo, R. Parra, J.A. Varela, M.M. Reboredo, M.A. Ramirez, M.S. Castro, J. Alloys Compd. 497 (2010) 349–353.
[25] M.A. Sulaiman, S.D. Hutagalung, M.F. Ain, Z.A. Ahmad, J. Alloys Compd. 493 (2010) 486–492.
[26] Z.H. Wu, J.H. Fang, D. Xu, Q.D. Zhong, L.Y. Shi, Int. J. Miner. Metall. Mater. 17 (2010) 86–91.
[27] D. Xu, X.N. Cheng, M.S. Wang, L.Y. Shi, Adv. Mater. Res. 79–82 (2009) 2007–2010.
[28] D. Xu, L.Y. Shi, Z.H. Wu, Q.D. Zhong, X.X. Wu, J. Eur. Ceram. Soc. 29 (2009) 1789–1794.
[29] D. Xu, L.Y. Shi, X.X. Wu, Q.D. Zhong, High Volt. Eng. 35 (2009) 2366–2370.
[30] S. Bernik, N. Daneu, J. Eur. Ceram. Soc. 27 (2007) 3161–3170.
[31] S. Bernik, S. Macek, A. Bui, J. Eur. Ceram. Soc. 24 (2004) 1195–1198.
[32] C. Leach, Z. Ling, R. Freer, J. Eur. Ceram. Soc. 20 (2000) 2759–2765.
[33] M. Peiteado, J.F. Fernandez, A.C. Caballero, J. Eur. Ceram. Soc. 27 (2007) 3867–3872.
[34] D. Xu, X.N. Cheng, X.H. Yan, H.X. Xu, L.Y. Shi, Trans. Nonferr. Met. Soc. China 19 (2009) 1526–1532.
[35] D. Xu, X.F. Shi, X.N. Cheng, J. Yang, Y.E. Fan, H.M. Yuan, L.Y. Shi, Trans. Nonferr. Met. Soc. China 20 (2010) 2303–2308.
[36] D. Xu, X.N. Cheng, H.M. Yuan, J. Yang, Y.E. Fan, L.Y. Shi, J. Alloys Compd. 509 (2011) 9312–9317.
[37] L. Ni, X.M. Chen, X.Q. Liu, R.Z. Hou, Solid State Commun. 139 (2006) 45–50.
[38] T. Li, Z.P. Chen, F.G. Chang, J.H. Hao, J.C. Zhang, J. Alloys Compd. 484 (2009) 718–722.
[39] J.N. Cai, Y.H. Lin, B. Cheng, C.W. Nan, J.L. He, Y.J. Wu, X.M. Chen, Appl. Phys. Lett. 91 (2007).
[40] L. Marchin, S. Guillemet-Fritsch, B. Durand, A.A. Levchenko, A. Navrotsky, T. Lebey, J. Am. Ceram. Soc. 91 (2008) 485–489.
[41] A. Tselev, C.M. Brooks, S.M. Anlage, H. Zheng, L. Salamanca-Riba, R. Ramesh, M.A. Subramanian, Phys. Rev. B. (2004) 70.